CHAPTER 5 COMPARISON OF ANALYSED ILDS

ILDs exhibiting similar thermal and colour properties are found in the chaotic terrains of Aram, Iani, Aureum, Arsinoes and Aurorae (Fig. 28). There are other chaotic regions nearby such as Pyrrhae, Margaritifer and Hydraotes Chaos that will not be dealt with here as they show no or hardly any exposures that could be analysed. Further to the west there are in the huge graben system Valles Marineris there are the most prominent and biggest ILDs either located in central, peripheral or enclosed troughs. Here the easternmost (Ganges and Capri/Eos) are studied.

In Chapter 4, 14 ILDs were analysed by their morphology, albedo, elevation, thickness, consolidation of materials, mineralogy and layering geometry.

In this chapter, all properties analysed will be compared and classified statistically in order to identify similarities and differences and deduce possible correlations.

Table 23: ILD parameters in comparison.

Locality	Morphology, Profile	Relative Albedo	Elevation [m]	Thickness [m]	Consolidation of Materials	Mineralogy	Layer Geometry [°]
Aram	Mesa, dome-like	Low	-3700±25 to -2900±25	Unit 1: 300±25 Unit 2: 500±25	High TI TI: Ø 461 SI ±50 (surrounding: Ø 372 SI±43) BT: 185-193°K (surrounding: 175-185°K) boulders and talus present	Kieserite + PHS within unit 1, haematite below unit 1 as erosional lack	-
Aureum 1	Irregular, mesa	Intermediate	-4600±12.5 to 4100±12.5	500±12.5	Intermediate TI TI: Ø 401 SI ±43 (surrounding: Ø 354 SI ±46) BT: 198-206°K (surrounding: 190-206°K)	No data	-
Aureum 2	Mesas and dome-like knobs, irregular	Low	-5100±25 to -3300±25	Unit 1: 850±25 unit 2: 950±25	Low TI TI: Ø 368 SI ±44 (surrounding: Ø 296 SI ±30) BT: 190-218°K (surrounding: 185-192°K) boulders and talus present	Unit 1: Kieserite and PHS, unit 2: spectrally featureless for CRISM, haematite below unit 1; nontronite within knobs but not associated with ILDs	-

Iani 1	Complex, dome-like	High	-4500±12.5 to -3400±12.5	1100±12.5	High TI TI Ø: 482 SI±77 (surrounding: Ø 344 SI±30) BT: 203-208 K (surrounding: 191-205 K) boulders and talus present	No data	-
Iani 2	Terrace-like, mesa	Intermediate	-3800±12.5 to -3000±12.5	800±12.5	Low TI TI Ø: 342 SI±52 surrounding: Ø 297 SI±28) BT: 195-203 K (surrounding: 187-195 K); boulders and talus observed	PHS and haematite	-

Iani 3	Terrace-like, dome-like	Intermediate	-4300±12.5 to -3000±12.5	1300±12.5	High TI TI Ø: 428 SI±41 (surrounding: Ø 308 SI±80) BT: 191-201 K (surrounding: 180-201 K) talus and boulders present	PHS and haematite	240±22/4±2 120±13/5±3
Arsinoes	Streamlined; dome-like	Low	-5200±25 to -3800±25	1400±25	Low TI TI Ø: 359 SI±82 (surrounding: Ø 333±39) BT: 180-203 K (surrounding: 180-195 K)	Spectrally featureless to CRISM (no iron-rich or hydrated minerals)	-
Aurorae	Butte, dome-like	Intermediate	-4600±50 to -3600±50	1000±50	Low TI TI Ø: 304 SI±40 (surrounding: 280 SI±33) BT: 185-197 K (surrounding: 178-182 K) talus and boulders present	Kieserite	-

Ganges 1	Mesa, dome-like	Intermediate	-4100±12.5 to -500±12.5	3600±12.5 Stair-steps of 500 m	Intermediate TI TI Ø: 424 SI±86 (surrounding: 327 SI±90) BT: 180-198 K (surrounding: 180-185 K) talus and boulders present	Kieserite up to -1900 m, PHS near the top at ~-500 m	4±2/4±3° below 9±5/255±36
Ganges 2	streamlined, dome-like	High	-4700±12.5 to -4000±12.5	Unit 1: 500±12.5 unit 2: 200±12.5	Intermediate TI TIØ: 385 SI ±51 (surrounding: 308 SI±43) no BT-data talus and boulders observed	Spectrally neutral, sulphates nearby	-
Ganges 3	Streamlined, dome-like	High	-4700±12.5 to -3700±12.5	unit 1: 400±12.5 unit 2: 600±12.5	High TI TI Ø: 498 SI±61 (surrounding: 387 SI±66) BT: 195-204°K (surrounding: 184-198°K) talus observed	No data 2 units identified	-
Ganges 4	Streamlined, dome-like	High	-4800±12.5 to -4200±12.5	Unit 1: 200±12.5 unit 2: 400±12.5	Intermediate TI TI Ø: 379 SI±38 (surrounding: 325 SI±32) BT: 185-195°K (surrounding: 174-185°K)	Spectrally featureless for CRISM,	-

					talus present		
Ganges 5	Streamlined, dome-like	High	-3800±12.5 to -3500±12.5	300±12.5	High TI TI Ø: 491 SI±68 (surrounding: 436 SI±80) BT: 203-215°K (surrounding: 196-205°K)	No data	-
Capri/Eos	Mesa, dome-like	Low	-5200±12.5 to -1700±12.5	Unit 1: -3300±12.5 unit 2: 200±12.5	Intermediate TI TI Ø: 388 SI±65 (surrounding: 364±85) BT: 184-204°K (surrounding: 183-192°K) talus and boulders present	Unit1: PHS + kieserite + haematite	65±27/5±3 47±32/7±3 34±16/18±12
		5 high, 5 intermediate, 4 low	**-5200 to -500**	**300-3600**	**5 high TI 5 intermediate TI 4 low TI**	**PHS+kieserite+haematite: 4 PHS+kieserite: 4 kieserite (only): 1 no above-named minerals: 3 No data: 4**	

5.1 MORPHOLOGY

On a large scale, ILDs occur as mesas (Aram, Aureum 2, Iani 2, Ganges 1, Capri/Eos) or mounds and buttes (Iani 1, Iani 3, Arsinoes, Aurorae, Ganges 2-5). These erosional morphologies (Fig. 36D, 41, 51C, 53D, 59B, cf. Sect. 2.4.3) indicate that their extent apparently was much greater than that observed at present. Moreover, surface structures such as pits (Aram, Iani 3, Ganges 2, Capri/Eos; cf. 46D), flutes and grooves (Aram, Iani 1, Arsinoes, Ganges 1-5; cf. Fig. 49D), and yardangs (Aureum 1, Iani 1, Iani 3, Arsinoes, Ganges 1, Ganges 5; cf. Fig. 46A) are the result of erosion by wind or water (Sect. 2.3.1, Sect. 4). Thus, flutes, grooves, and pits yield insights to the erosional regime and the affected material. ILDs show variable resistance to erosion indicated by the presence of the named erosional features, which confirm there are different materials and irregularities within ILDs. The top of all ILDs appears massive since layering in the upper parts is small in scale and therefore only visible in HiRISE and a few MOC images whereas lower parts show large-scale layering (e.g. Fig. 30D, 31D, 35, 36A, 49D). Actually thickly bedded lower and finely layered upper parts are observed within ILDs suggesting changes in the depositional or erosional conditions e.g. Aureum 2 (cf. Sect. 4.1.2, Fig. 37D).

A thin dark mesa unit, previously described by *Malin and Edgett* (2000), is present on the ILD surface of at least 4 ILDs (Aureum 1, Aureum 2, Ganges 1+5; Fig. 57G). These observations indicate that after ILD deposition a mantling process covered them and erosion exhumed them later on. Thus the thin mesa unit most likely is a result of erosion of the mantling unit and ILD material below. All ILDs show a stair-stepped morphology - implying alternating strata of competent and incompetent material - observed at different scales (e.g. Fig. 36F, 49D, 51C, 53D). It suggests episodic deposition of competent and less competent material and therefore material differences.

Convoluted-like strata are observed within ILDs in Aureum 2, Iani 1, Ganges 1 and Capri/Eos (e.g. Fig. 37D) resembling convoluted bedding. It indicates dehydration structures which occur in fine-layered silts and fine-grained sands of low permeability on Earth [*Füchtbauer*, 1988]. There, the whole sediment is exposed to movement in layers, which sink in irregularly, forming sharp crests and broad troughs. In general, restricted dehydration requires fast sedimentation to retain the interstitial water. However, once precipitated evaporite mineral grains may be exposed to the same physical processes of erosion, transport and deposition that are known from siliciclastic and carbonate depositional environments [*Reading*, 1996], and thus form sedimentary bedforms. Therefore, similarities to those sedimentary structures do not necessarily point to the aforementioned materials but do indicate deposition under sub-aqueous conditions. All named morphologies (yardangs, flutes, grooves, pits) point to erosion by water and wind, which was present during and/or after the times ILDs formed, at most in the Late Hesperian and Amazonian (Table 2, 3, Sect. 2.4.3, 5.8). Moreover, differences in the consolidation of material and possibly its composition are indicated by stair-stepped morphologies. Some small-scale folding has been observed within layers, especially in Ganges 1, Ganges 2 and Iani 1. As hydrated sulphates were found at least in Ganges 1 (cf. Fig. 53F, 53G, Table 17), these features may be explained by intense deformation during the accumulation of the deposit. In this instance, changes in volume may be related to

dissolution and the growth of crystals by dewatering and water absorption. Sulphates as well as salts show a mechanical behaviour of soft material under ambient or low temperatures (T< 200°C) which may result in soft deformation [e.g. *Warren*, 2006].
The occurrence of these features in Iani 1 (Sect. 4.1.3) of which the mineralogical data are lacking, and Ganges 2 (Sect. 4.2.1), which is spectrally neutral and therefore lacks hydrated and iron-rich minerals (Sect. 3.2.2), could indicate the presence of anhydrous sulphates (e.g. anhydrite) or salts (e.g. halite) that lack absorptions in the VNIR, but is highly theoretical.

MOC images show ILDs exhibit differences in the surface morphologies observed on their tops (Fig. 60), where two morphological types can be found:
Type 1 occurs on the top of Ganges 2-5 and Iani 1. These ILDs are heavily fractured, eroded and in Ganges 3 and Ganges 4 exposed as dissected blocks (Fig. 55A, 56A). It is characterised by

- A massive and rough appearing surface that is heavily fluted and grooved,
- shows a high to intermediate albedo (Sect. 3.2.1),
- an intermediate to high TI (Sect. 3.2.2) and is present on ILDs that show
- no hydrated sulphates and iron-rich minerals (Ganges 2, Ganges 4; Tables 18, 20) or on those where the mineralogy is unknown (Iani 1, Ganges 3, Ganges 5; Tables 12, 19, 21).

Type 2 (Fig. 60) appears on the top of ILDs in Aram, Aureum 1+2, Iani 2+3, Arsinoes, Aurorae as well as in Ganges 1 and Capri/Eos (Fig. 61) and is characterised by

- a dissolved-looking surface that exhibits surface vugs and sharp-edged crests. These vugs reveal underlying strata unless they are either covered by windblown material.
- A low to intermediate albedo (Sect. 3.2.1),
- a low to high TI and is present on ILDs that show
- hydrated sulphates (Aram, Aureum 2, Iani 2+3, Aurorae, Ganges 1, Capri/Eos; Tables 9, 11, 13, 14, 16, 17, 22) no hydrated sulphates and iron-rich minerals (Arsinoes; Table 15) or on those where the mineralogy is not known (Aureum 1, Table 10).

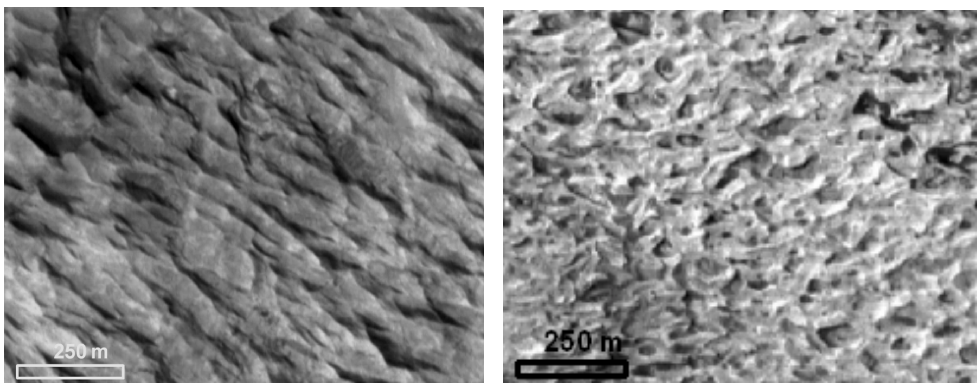

Figure 60: Distinguished surface morphologies. Two different surface morphologies have been observed on ILDs. *(left)* Surface type 1 showing an 'adjusted' surface structure probably highly affected by wind erosion (Sect. 2.3.1), as indicated by grooves and flutes. Layering in the upper more light-toned part is extremely fine (MOC orbit R0900025). *(right)* Surface type 2 displays surface vugs and sharp-edged crests (MOC orbit

E2000998). Surface depressions exhibit dark windblown material in both cases.

To find out whether these different morphologies are restricted to a certain area, they were plotted on a topographic map (Fig. 61). Obviously, these morphologies show no correlation to a certain topographic locations since both types occur in chaos as well as chasma regions. However, surface type 1 (white crosses in Fig. 61) seems to be associated with regions that are highly affected by water erosion since they are located near the discharge regions. Iani 1 is near Ares Vallis, Ganges 2-5 near Aurorae that empties into Hydraotes (2°N/325°E) and Arsinoes is also connected there. Apparently, surface type°2 is more often observed in protected areas where there was lower discharge.

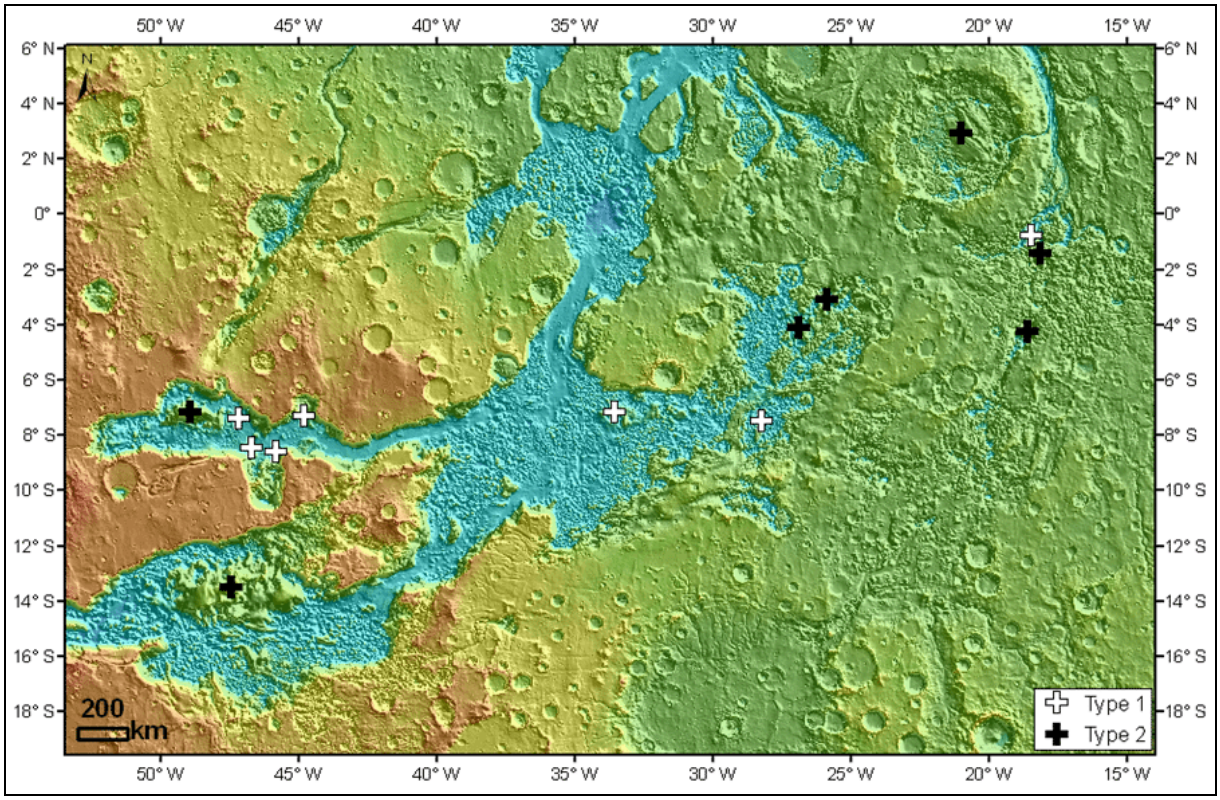

Figure 61: MOLA map of the research area showing the two different surface morphologies. Compare Fig. 28 for locations. White crosses correspond to surface type 1, black crosses correspond to surface type 2 (Fig. 60), which seems to correlate with sulphate detections (Sect. 5.6). Both types occur in the eastern chaotic terrains and the chasmata whereupon type 2 seems to be associated with areas that are more protected and type 1 with discharge areas that are more affected by erosion.

5.2 RELATIVE ALBEDO

As already mentioned in section 3.2.1, the relative albedo was established based on grey-scale values and classified into low medium and high relative albedo (Fig. 62). ILDs with a low albedo are found in Aram, Aureum 2, Arsinoes, and Capri/Eos (Tables 9, 11, 15, 22) whereas ILDs of an intermediate albedo are present in Aureum 1, Iani 2, Iani 3, Aurorae, and Ganges 1 (Tables 10, 13, 14, 16, 17). ILDs with a high albedo are located in Iani 1 and Ganges 2-5 (Tables 12, 18-21; cf. Fig. 61). Effects of coverage by aeolian material (dust, sand) were taken into account while estimating the albedo classes. A high albedo appears on ILD surfaces that show slight coverings of dark aeolian sands and are true for 36% of the ILDs (Fig. 62). ILDs with low albedo have the thickest covers of aeolian materials (28%). Intermediate albedo is present to 36% of the ILDs. ILDs with a high albedo correlate with surface type 1 (Fig. 61) mentioned in the previous Sect. 5.1.

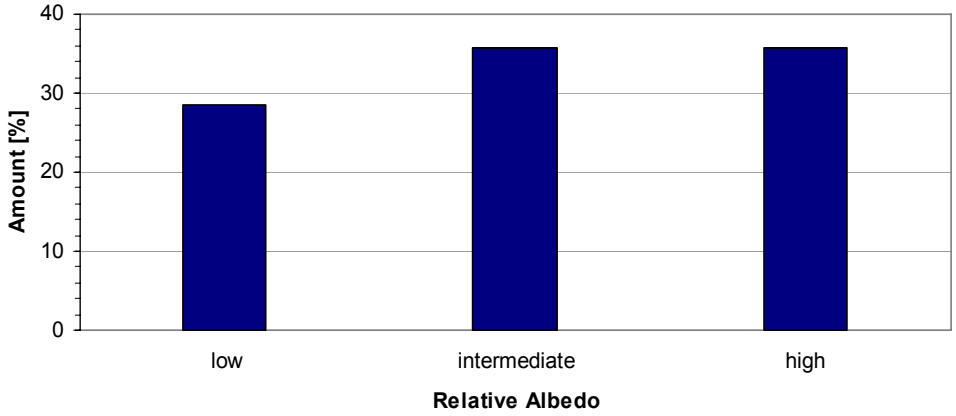

Figure 62: Diagram showing the classification into low intermediate and high albedo. Predominantly, ILDs have high and intermediate albedo. Only 28% of ILDs show a low albedo. Low may be explained by coverings of dark aeolian material. Conversely, ILDs of surface type 1 - (Sect. 5.1, Fig. 60, 61), tend to display high albedo and ILDs that show type 2 have low to intermediate albedo.

5.3 ELEVATION

ILDs can be found at elevations below the level of the surrounding plateau (Fig. 63, 64). They are exposed at different locations in the chasmata (marginal parts, centre of the canyon floor) as well as in craters and other depression that exhibit chaotic terrain (Fig. 28). Not all these locations are in the deepest regions (Fig. 63). Their heavily eroded nature as well as ILD fragments that are found near each ILD and on chaotic terrain remnants suggest that their extent once was much greater than it is now.
ILDs occur at elevations from -5200 m to -500 m (Fig. 63-65). This coincides with the elevation ranges of ILDs in Valles Marineris. In chaotic terrains, ILD elevation ranges from –5200 m to -2900 m (Aram). The highest elevation of all ILDs is observed at the top of Ganges 1 at -500 m (Fig. 65). And the lowest is observed at the top of Ganges 4 with -4200 m (Fig. 65, Table 20). The base level for ILDs is in Arsinoes and Capri/Eos at -5200 m (Fig. 65, Tables 15, 22).

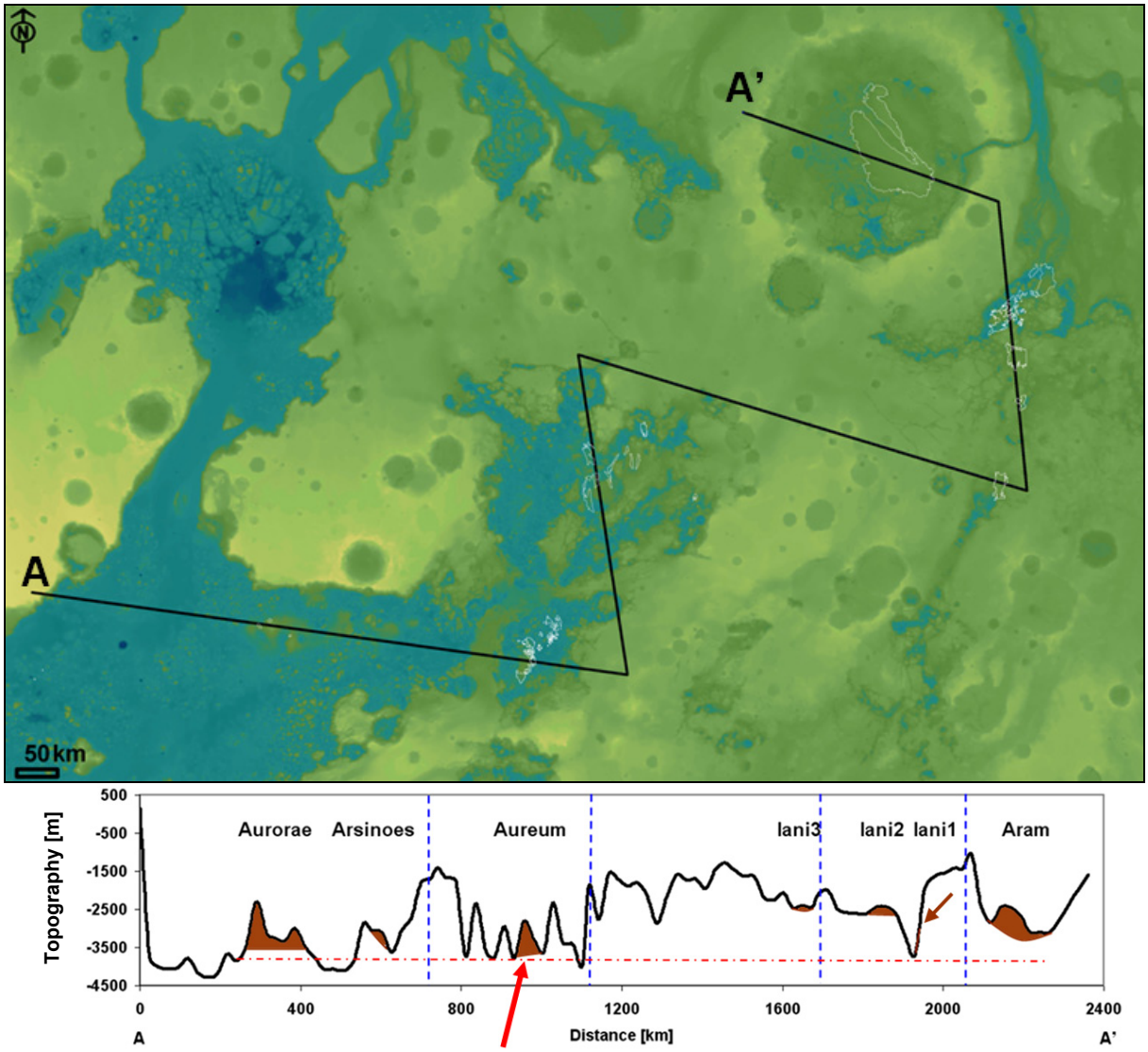

Figure 63: Profile of ILD elevations for the eastern chaotic terrains in comparison. *(top)* MOLA DEM showing location of cross-section A-A' covering ILDs in the chaotic terrain. ILDs are outlined white. In addition they are indicated by arrows. (*bottom*) Cross-section showing the extent of ILDs along the profile marked by regions. Blue dashed lines indicate breaks in the profile (cf. Fig. above). The dashed red line marks the minimum elevation (base level) at which ILDs are exposed along the profile; here with Aureum 2 as reference marked by a red arrow. The location of Iani 1 is indicated by a brown arrow. Note that Aureum 1 is not covered by the profile. Absolute elevations for each ILD in general were determined by HRSC-DTMs (Sect. 3.2.3). Accuracy: Distance ±0.463 km, topography ±2 m (Sect. 3.2.3).

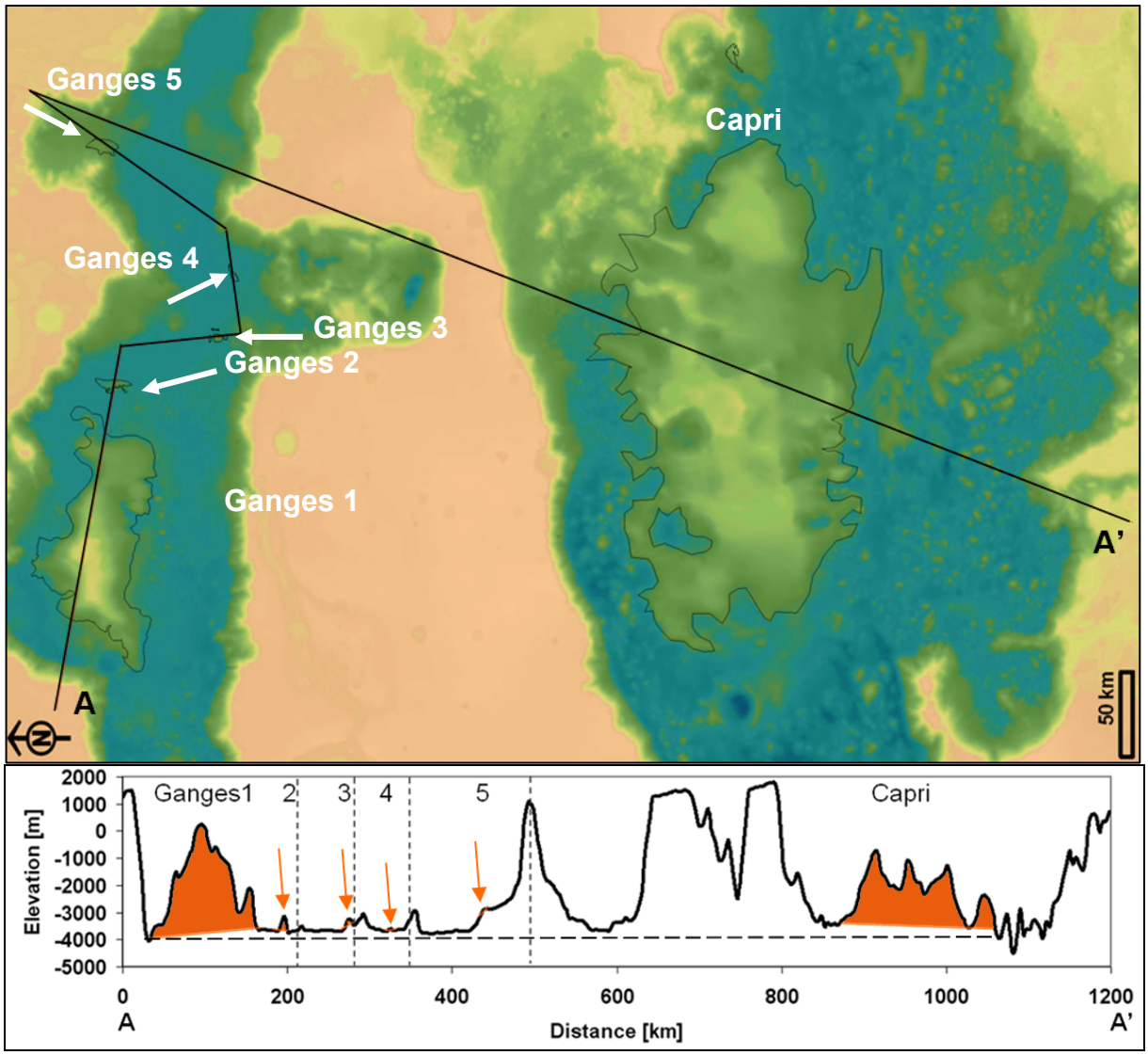

Figure 64: Profile of ILDs in the chasmata in comparison. *(top)* MOLA DEM showing location of cross-section A-A' covering ILDs in Ganges and Capri/Eos. ILDs are outlined black. In addition the smaller exposures (Ganges 2-5) are indicated by white arrows. *(bottom)* Cross-section shows the extent of ILDs along the profile indicated by orange regions. The dashed lines mark breaks in the profile (cf. Fig. above). In general, ILDs seem to be exposed in the same elevation range, but some are obviously weaker and more susceptible to erosion (see Ganges 2-5, indicated by arrows). The dashed horizontal line shows the minimum elevation at which ILDs are exposed, here with Ganges 1 as reference. Note that the absolute elevations for each ILD were determined from HRSC DTMs (Sect. 3.2.3). Accuracy: Distance ±0.463km, topography ±2m (Sect. 3.2.3).

Some ILDs show different morphological units (Tables 9-22). These in turn are ascribed to certain elevations. As the occurrence of hydrated minerals such as kieserite, gypsum and PHS indicates hydration, water may have been present up to a certain elevation.

The maximum elevation of hydrated sulphates corresponds to a region near the top of Ganges Mensa (~-500 m; Table 17) for the chasmata and Iani Chaos ILDs (-3000 m; Table 13, 14) for the eastern chaotic terrains. This in turn indicates ILDs are in parts sulphate bearing up to the top, so the original uppermost elevation that experienced hydration could be higher than measured. Overall, hydrated units (Fig. 65) are mainly present in the close proximity to outflow channels and occur within ILDs that are affected by rock break-up (Fig. 69) and ILDs that show surface type 2 (Fig. 60, 61). The correlation of

hydrated ILDs with the close proximity to outflow channels could indicate the prolonged presence of water to form hydrated sulphates. However, as seen in figure 65, a low ground elevation as it is present in Ganges 2, Ganges 4 and Arsinoes does not assure the presence of hydrated minerals.

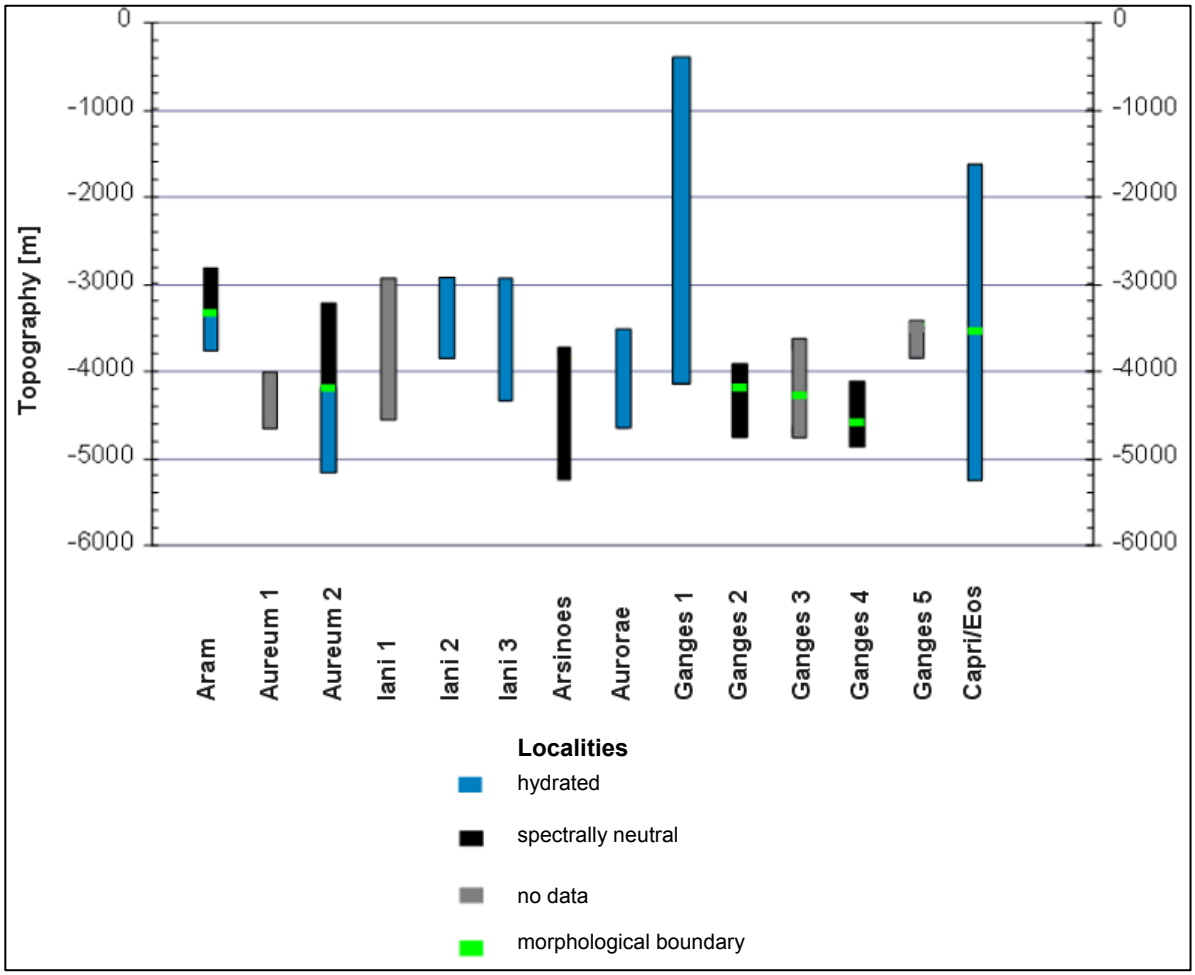

Figure 65: Diagram showing the extent of hydrated units within ILDs in elevation. Overall hydrated minerals were detected between -5200 m to -500 m within chasmata. In chaotic terrains, hydration is found from -5100 m to -3000 m. Hydration boundaries correlate with the morphological differences between units within ILDs described in Sect. 4. Their upper unit mostly corresponds to spectrally neutral cap rock (cf. Fig. 60, 61, Sect. 5.1). ILDs that show a spectrally neutral upper unit sometimes show a hydrated lower unit (e.g. Aram, Aureum 2), are strongly affected by weathering and mostly are located in protected regions (cf. Fig. 61, 68, 69). Topography is based on HRSC DTMs (Sect. 3.2.3). For accuracies, see Tables 9-22 (Sect. 4).

5.4 THICKNESS

Thickness measurements were performed (Sect. 3.2.3) for each ILD (Fig. 66). Varying thicknesses assuming ILDs have horizontal strata are also identified. ILDs in chasmata (Ganges and Capri Mensa) have a much higher mean thickness (<3600 m) than those in chaotic terrains (<1500 m; Sect. 5.3, Fig. 65). A possible correlation between thickness could show thickness and geographic location (i.e. chasma or crater) are correlated. One of the formation hypotheses for ILDs is the pyroclastic deposit hypothesis (Sect. 1, 2.4.3, 6.2). ILDs may be pyroclastic deposits derived from Tharsis volcanism (Table 4).

Pyroclastic fall deposits show decreasing thicknesses with increasing distance to their source area [*Tucker*, 2001], thus a correlation of thickness and geographic location could indicate ILDs have the same volcanic source. However, as shown in Fig. 65, there is no clear correlation between thickness and geographic location. ILDs in the chasmata (Ganges 2-5) show thicknesses comparable to ILDs in the eastern chaotic terrains. Based on the assumption, ILDs are pyroclastic fall deposits, then erosion should have lowered their thicknesses to blur this correlation or they should have different sources. A remarkable high thickness is present in both Ganges 1 and Capri Mensa.

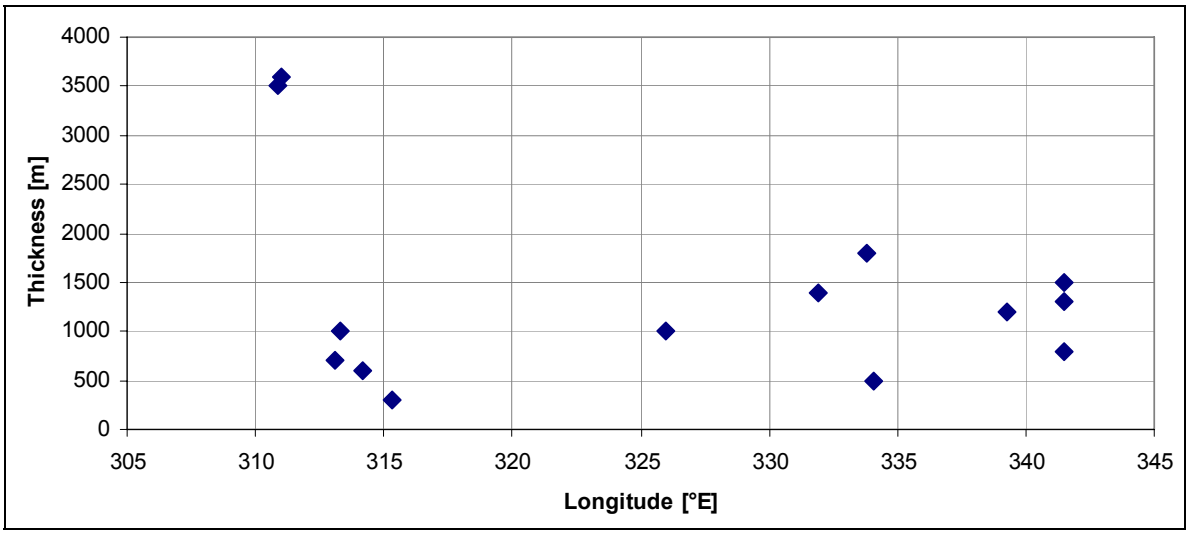

Figure 66: Diagram showing thickness vs. longitude. Thicknesses are very high in both Ganges (1) and Capri Mensa (3500-3600 m). In all of the other ILDs, they are below 1200 m (300-1400 m) and therefore in the same range. Obviously, there is no clear correlation between thickness and longitude. For the case of pyroclastic deposits, ILDs either have experienced heavy erosion to blur this correlation or have different source areas. A possible correlation between ILDs in Valles Marineris is conceivable, as there is a decrease in thickness; however, the ILDs are very close to each other.

Some ILDs in parts show different morphological units that are found again in other ILDs (Sect. 4). Especially their top, which is in parts a spectrally neutral low albedo, massive-appearing cap rock, is comparable (Fig. 60, 61). On a higher resolution (MOC, HIRISE, Table 8), this cap rock even shows layering (Fig. 36F). It is characterised by surface vugs, sharp-edged crests and a small-scaled stair-stepped morphology indicating material differences (Sect. 5.1). The cap rock therefore coincides with surface type 2 (Fig. 60) described in section 5.1. However, Ganges 2-4 (Sect. 4.2.1) are different. Their cap unit features a higher albedo than their lower units and finely layered textures (Fig. 54D).
Mostly 1 unit was identified within ILDs but there apparently is another one, indicated by stair-stepped morphology and competent strata producing boulders and talus (Sect. 5.5, 5.1).

5.5 CONSOLIDATION OF MATERIALS

TES TI (Sect. 3.2.2) reflects the physical properties of the surface and is therefore affected by material properties such as density, heat capacity and thermal conductivity (Sect.

3.2.2). Nighttime surface temperatures are used to observe the TI of the material relative to its surroundings (Sect. 3.2.2). A high TI indicates a more consolidated, coarse material that appears as bright regions (Sect. 3.2.2). It reaches higher surface temperatures, and retains heat for a much longer time. THEMIS BT (Sect. 3.1.6, Table 8) is closely related to TI (Sect. 3.2.2). Dark regions show lower surface temperatures and TI as they correspond to unconsolidated, dusty, fine-grained material that cools off much faster during nighttime.

The mean TI measured on ILDs ranges between 304 and 498 SI (Fig. 67, 68). A thermal inertia of >386 SI indicates rocks, bedrock, duricrusts and polar ice whereas a thermal inertia of 140-386 SI indicates sand, rock, bedrock and some duricrusts [*Putzig et al.*, 2005]. The ILDs that show the highest TI of 428-498 SI are those in Aram, Iani 1, Iani 3, Ganges 3, and Ganges 5 (Tables 9, 12, 14, 18, 19, Fig. 68). The ILDs of Aureum 2, Iani 2, Arsinoes, and Aurorae rate lowest (Tables 11, 13, 15, 16, Fig. 68). Intermediate TI was observed in Aureum 1, Ganges 1, Ganges 2, Ganges 4 and Eos/Capri (Tables 10, 17, 18, 20, 22, Fig. 68). A high TI is mostly present in ILDs of high albedo (Sect. 5.2, Iani 1, Ganges 3+5) which are ILDs that are located in discharge regions of outflow channels and are heavily fluted and grooved (type 1, Sect. 5.1).

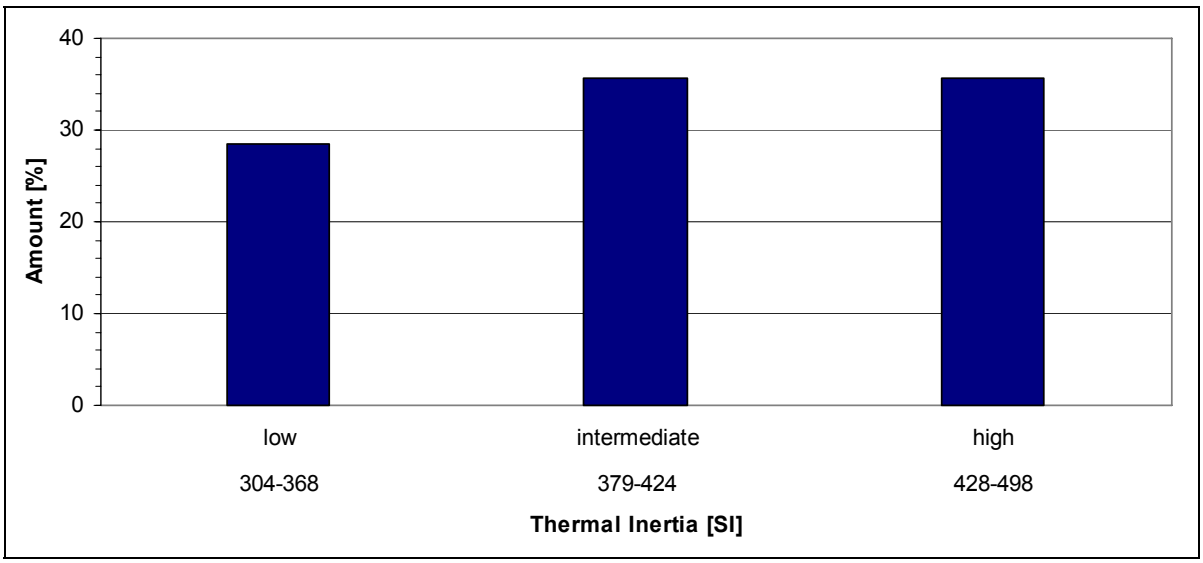

Figure 67: TI classification. As described in section 3.2.2, TI was classified into low, intermediate and high. High and intermediate TI is present to 36% of the ILDs respectively and low TI to 29% (cf. Fig. 68).

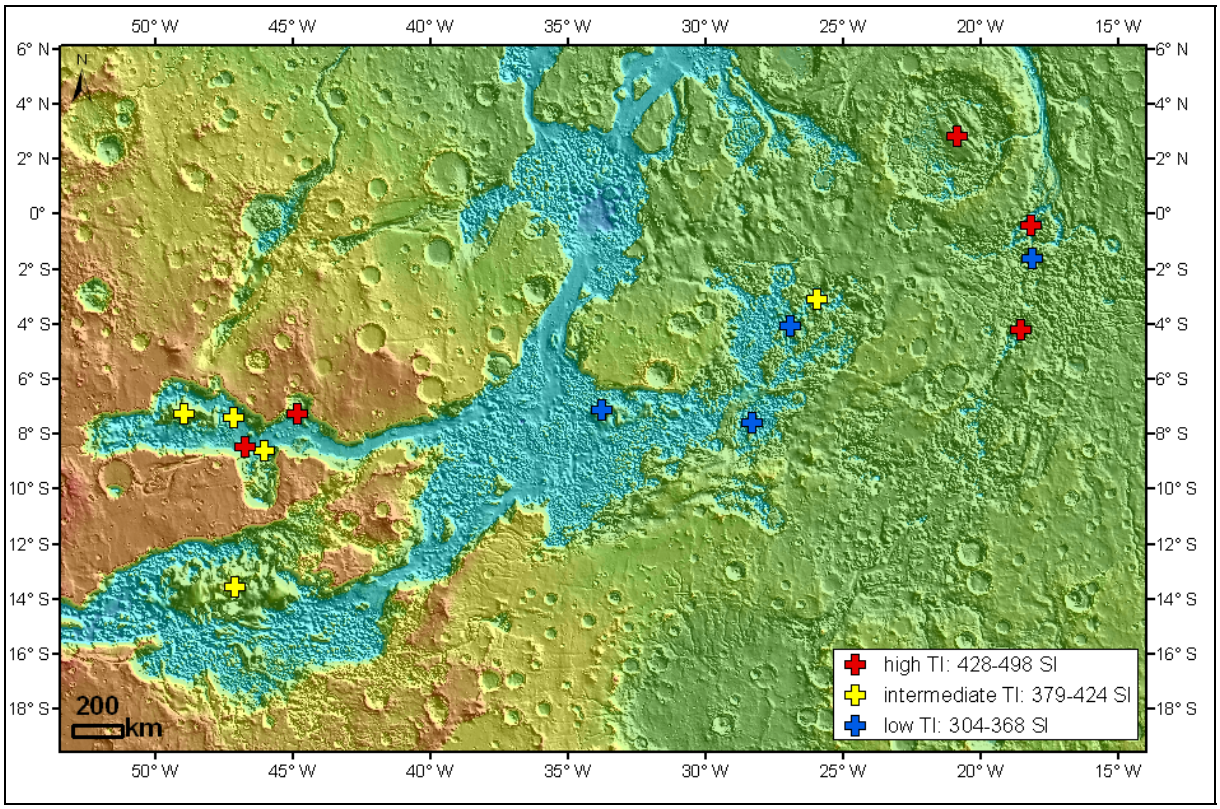

Figure 68: TI and geographic location. ILDs were classified into TI groups (Fig. 67, Sect. 3.2.2), which are shown here in their geographical context. Red crosses correspond to high, yellow to intermediate and blue to low TI. Low TI is concentrated in the eastern chaotic terrains. High TI occurs in chasmata as well as in the chaotic terrains as do intermediate TI. However, chasma ILDs show intermediate to high TI but no low whereas the chaotic terrains incorporate all three classes.

At the base of steep ILD slopes, meter-sized boulders and talus are present. Observed on HiRISE images, they indicate weathering of strata (cf. Fig. 59A, 31A, 36E, 36F, 43F) and well-consolidated material. Apparently, the level of break-up differs between ILDs (Fig. 69). There are ILDs like Ganges 1, Iani 1, Iani 2, Iani 3, Aram, Aureum 2, Capri Mensa, and Iani 3 that are highly affected by rock break-up (group 1), while others, such as Aurorae, Ganges 2 and Ganges 5 appear hardly affected (group 2). However, the level of break-up is not known for Arsinoes, Aureum 1, Ganges 3, and Ganges 4 due to the lack of suitable HiRISE images. On the one hand, differences in the level of rock-break up may be explained by assuming a smaller scale of break-up for group 2, indicating higher compaction which retains material and/or finer material removed previously.
Thus, group 1 could be is weaker and therefore more affected by rock-break-up. Since, highly affected ILDs may be associated with lower TI, in contrast to hardly affected ILDs. Unfortunately, the classification into ILDs highly affected by rock break-up (group 1) and hardly affected by the same (group 2) does not correlate with the TI classification (Fig. 68, 69). In addition, there is a slight correlation with the surface types (Sect. 5.1, Fig. 60, 61) in that ILDs of group 1 (Fig. 69) belong to surface type 2 (Fig. 60, 61), whereas group 2 can be ascribed to surface type 1 (Fig. 60, 61, 69). Besides, mineralogy correlates with sulphate-rich ILDs and thus with the surface types. Since frost weathering may be considered for rock break-up, it would explain the named correlation: Volume increase due to freezing of water inside the rock results in rock break-up into talus and boulders.

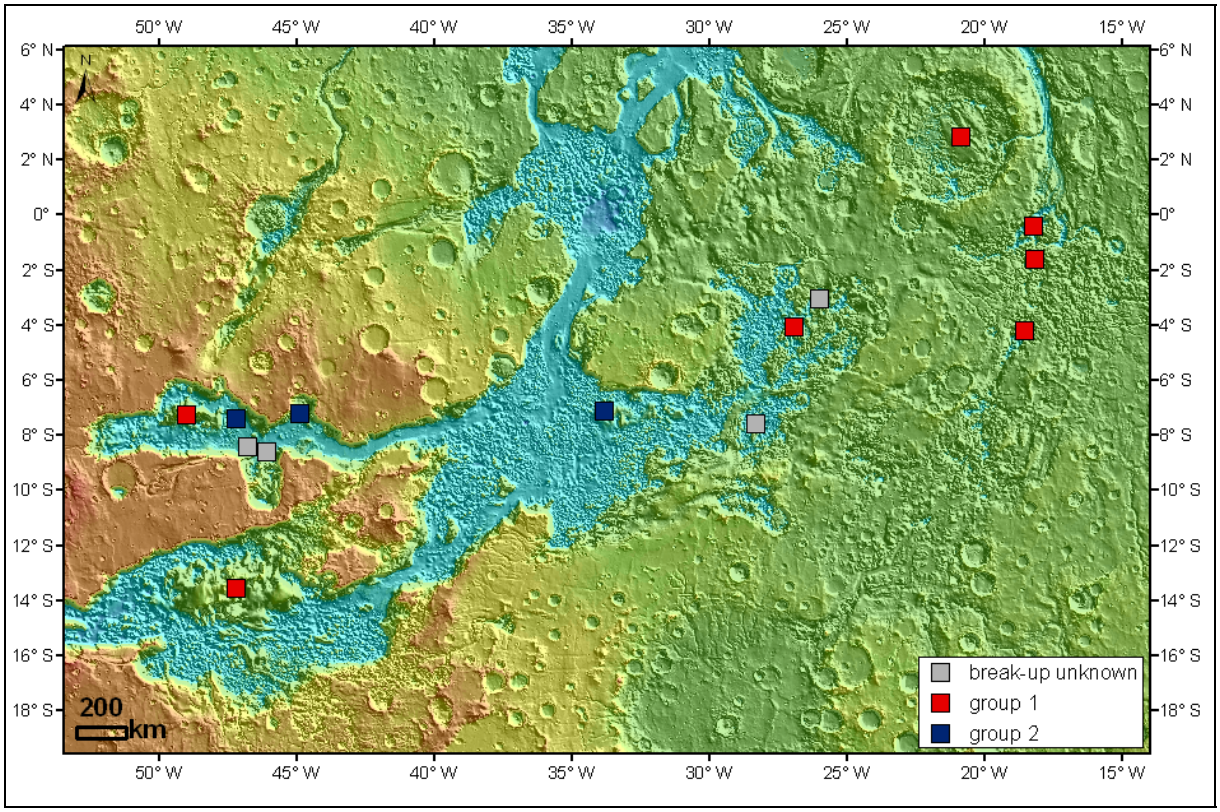

Figure 69: MOLA-map showing a classification by rock break-up of ILDs in a geographical context. For location names, see Fig. 28. Grey boxes correspond to regions where rock-break-up is unknown. Red boxes indicate ILDs that are highly affected by rock break-up (group 1) and blue boxes are ascribed to ILDs that are hardly affected by rock break-up (group 2). ILDs in the close vicinity of outflow channels or discharge channels such as Ganges 1, Capri and Iani 1-3 are greatly affected by rock break up (group 1), whereas ILDs that are more protected from erosion show hardly any effects. Moreover, surface type 2 also correlates with group 1 (Fig. 60, 61) as well as the hydrated mineralogy (Fig. 69).

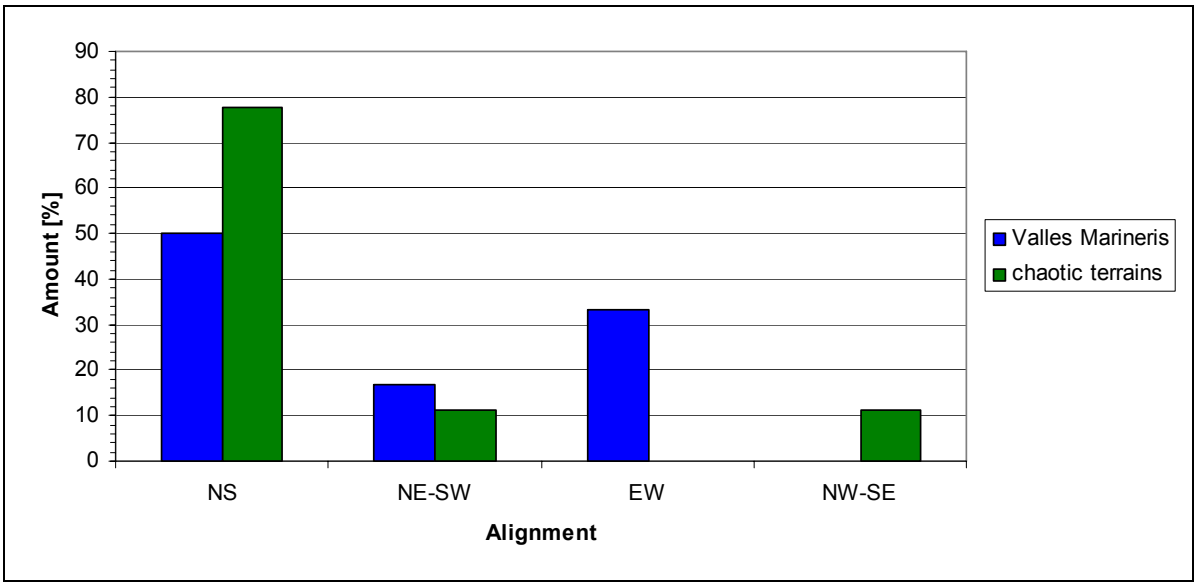

Figure 70: Diagram showing the statistic orientation of ILDs in Valles Marineris and chaotic terrains. In Valles Marineris, the largest ILDs of Ganges 1 and Capri Mensa follow the EW-trending chasmata in their elongation (33 %) whereas the majority (Ganges 2, Ganges 3, Ganges 5) is NS-aligned. In chaotic terrains ILDs mostly (>78 %) show a NS-alignment. Their shapes may indicate preferred directions of erosion by wind or water. Consequently, in both regions NS-trending erosional structures are observed.

5.6 MINERALOGY

In HiRISE false colour images, differences in composition are conspicuous. ILDs are yellow, mafic sands are blue and dust is brown (e.g. Fig. 30D). ILD talus mostly is brownish whereas boulders are yellow. Minerals require certain eh, pH, temperature and pressure conditions for their formation (Sect. 1, 3.2.2). They therefore reveal the climatic conditions that dominated during their formation. MEX OMEGA, MRO CRISM and MGS TES (Table 8) measurements show that sulphates (kieserite, gypsum[1], PHS) and haematite are present in ILDs in many locations of the research area [e.g. *Glotch and Christensen*, 2003; *Gendrin et al.*, 2005; *NoeDobrea et al.*, 2008]. These minerals point to aquatic conditions. Sulphates form by evaporation due to decreasing water availability or by hydrothermal alteration of volcanic material [Matthes, 2001], suggesting a warmer, more humid Mars and acidic conditions during the formation of sulphates, which is assumed to have taken place in the Hesperian (Fig. 3, Sect. 2.1).
In general, sulphates were detected on high-albedo scarps with slopes of >10° that are less covered by aeolian material. Kieserite was found on steep, high-albedo, thickly bedded outcrops of high TI in Aram, Aureum 2, Aurorae, Ganges 1 and Capri/Eos (Fig. 37A, 37B, 37D, 53D-F, 53I, Sect. 4). It appears massive but features a stair-stepped morphology (Sect. 5.1), indicating different materials in between. The unit in which it is exposed (Sect. 5.1, 5.4) features boulders and talus as well as angular edges that indicate weathering and rock break-up (Sect. 5.5).
PHS were detected interlayered with kieserite. They mostly show a lower albedo, are smoother in appearance, distinctly layered and more slope-forming and were found in Aram, Aureum 2, Iani 2+3, Ganges 1 and Capri/Eos (Fig. 38A, 38B, 53D, 53G).
Haematite-rich layers mostly occur below sulphate-rich strata in the form of eroded, low-albedo units (Aram, Ganges 1, Aureum), or else they coincide with these strata (Iani 2+3; Sect. 4.1.1, 4.1.2).
Some ILDs show sulphate minerals while others do not (Fig. 71), e.g. ILDs (Ganges 2+4) in Ganges Chasma (Fig. 54A, 56A) and Arsinoes (Fig. 48). There, no spectral signature is detectable even by the high-resolution CRISM instrument (Sect. 3.2.2). This implies that their surface, which obviously is freshly eroded, does not contain iron-bearing and/or hydrated minerals. This may indicate the presence of other sulphates such as anhydrite or even halite, sylvite or silica minerals (e.g. plagioclase) that are featureless in the spectral range of CRISM (Table 8).

During the formation of sulphates and haematite, aquatic conditions dominated.

- The presence of gypsum indicates temperatures <60°C and a positive oxidation potential. It may have formed as a result of evaporation in a depression (e.g. chaotic terrain) or secondarily by water absorption of pre-existing anhydrite, a direct indicator of volcanic activity.
- Kieserite is associated with comparable temperatures of 30 to 50°C. Formation by evaporation or by alteration during subsurface circulation is rather more likely

[1] Previous mineral detection for Iani 2+3 pointed to gypsum (Sect. 4.1.3).

than by dehydration of PHS (Sect. 3.2.2). Moreover, the sites where kieserite has been detected (steep slopes, fresh, eroded) suggest that it is very probably not a dehydration product of PHS. In addition, kieserite indicates acidic pH-conditions compared to PHS.

- PHS may have formed as a product of kieserite weathering by water absorption. Since it occurs interlayered with kieserite, and the two form under different conditions, at least part of the PHS could have been generated by the hydration of kieserite exposed at the surface for prolonged periods (Sect. 3.2.2).
- Haematite was found within sulphate-rich units and as a residual lag at their base, suggesting it was eroded out of the ILDs (Sect. 3.2.2).

On Mars, haematite is assumed to have formed by precipitation in large lakes or hot springs (during ancient Tharsis volcanism), as a residue when water leached away other minerals, or by chemical alteration of volcanic ash deposits (Sect. 3.2.2). In general, it does not require water for its formation as it may be generated by dry, thermal oxidation processes (Sect. 3.2.2). It is assumed to have originated in the Amazonian (Table 3, Fig. 3, Sect. 2.1) and indicates a warmer, more humid Mars during its formation.

An interesting aspect is that comparing observed surface morphologies (Sect. 5.1, Fig. 60, 61) and mineralogies (Fig. 65, 71) yields an apparent correlation. CRISM/OMEGA detections of sulphates mainly correspond to surface type 2 (Fig. 60, 61), whereas ILD surfaces that are neutral to these instruments (Fig. 61, Sect. 3.2.2) mainly correlate with surface type 1 (Fig. 60, 61, 71). Hydrated ILDs (Fig. 71, 65) are also associated with group 1, which is heavily affected by rock break-up and occurs in close proximity to outflow channels (Sect. 5.5, Fig. 69). In any case, ILDs that are spectrally neutral feature freshly eroded surfaces (Sect. 5.2, Fig. 61), unlike ILDs where sulphates were detected that show cap rock often covered by sands (Sect. 5.1). This may be due to material that is more disrupted and eroded as these ILDs occur mostly in unprotected areas (Fig. 65, 71, 60), and are heavily fluted and grooved (Fig. 60).

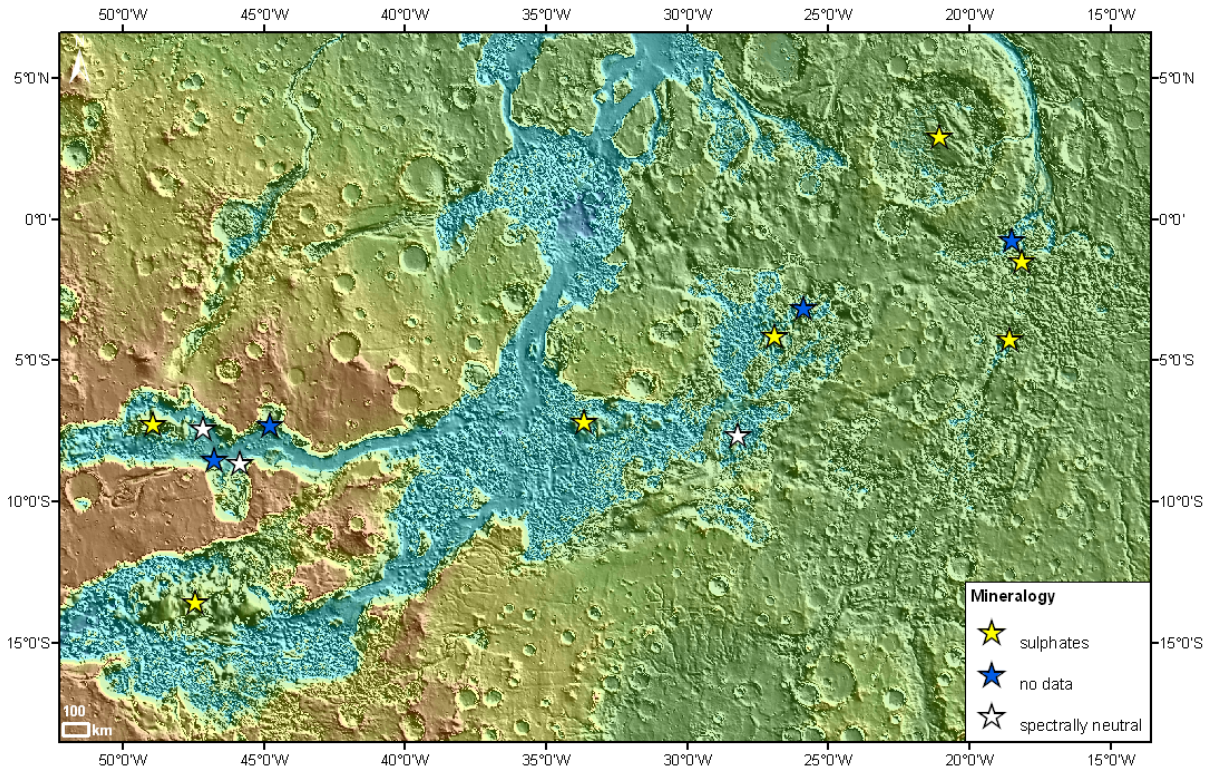

Figure 71: MOLA map showing regions where sulphates were detected by OMEGA and CRISM. Yellow asterisks correspond to sulphate finds that mainly correlate with surface type 2 (Fig. 60, 61, Sect. 5.1), group 1 (Fig. 69, Sect. 5.5), which is heavily affected by rock break-up. Note the close proximity to outflow channels and areas were sulphates were found. Spectrally neutral surfaces, indicated by white asterisks exhibit surface type 1 (Fig. 60, 61). Blue asterisks mark locations for which spectral information is lacking.

Observations at Meridiani Planum

Meridiani Planum is located east of Iani Chaos at 0.9°N/357°E (Fig. 10, 28). Several researchers have studied the local layered deposits that coincide with sulphate- and haematite-rich exposures [*Christensen et al.*, 2000a; *Hynek et al.*, 2002; *Lane et al.*, 2002; *Chan et al.*, 2004; *Christensen and Ruff*, 2004; *Glotch et al.*, 2004; *Ormö et al.*, 2004; *Squyres et al.*, 2004; *Arvidson et al.*, 2005; *Clark et al.*, 2005; *Glotch et al.*, 2006; *Andrews-Hanna et al.*, 2007b; *Griffes et al.*, 2007]. At Meridiani, the haematite-rich unit is overlain by sulphates and may have formed by erosion of material and aeolian sorting into sand dunes at the foothills or scarps [*Mangold et al.*, 2007]. Sulphates are associated with the 'etched and pitted terrain', which is eroded layered material. A minor amount of Fe-rich clay minerals is also present in these sulphate-rich outcrops. Hence, this local association of clay and sulphate may point to conditions different from those strongly acidic fluids expected at the Opportunity landing site.

The distribution of sulphates and haematite in layered deposits indicates that comparable aquatic conditions also dominated in regions outside of chaotic terrains and Valles Marineris and that mineral detection from orbiters is consistent with ground observations. Based on the stratigraphic relationship of haematite, *Glotch and Rogers* (2007) assumed a hydrological cycle lasting from the Late Noachian to the Late Hesperian (Table 3) which reached from Meridiani Planum via Aram Chaos to Valles Marineris and haematite

formation at neutral pH-values.

5.7 LAYER GEOMETRY (STRIKE AND DIP)

To obtain information about the internal geometry of the ILDs, strike and dip measurements were performed (Sect. 3.2.3) which also permit the distinction between volcanic or sedimentary formation, provided that post-depositional tilting is ruled out (Sect. 3.2.3).

In Iani Chaos, strike and dip measurements revealed sub-horizontal layering, as layers dip at less than 10° to the west in the western part and to the east in the eastern part. The change in dipping direction is caused by an antiform that is partially eroded (Fig. 45E, 46A). Ganges 1 (Fig. 53J) also shows slightly inclined layers that dip downslope at less than 10°: sub-horizontal layering was assumed there as well. Its northern part is slightly more inclined (and less steep) than the southern as seen in Fig. 53K (constructed from outcropping layers) which could be due to weathering. Similarly the southern part shows a mantling which protects from weathering. Conversely, a dip of 5-18° (downslope) has been observed in Capri Mensa which indicates the inclination of the strata was possibly caused by rock break-up. The whole ILD is much disrupted which may be due to its location in a discharge area, experiencing multiple erosional events and possibly ponding. Outward dipping cannot be excluded there since the lower part of the ILD is more inclined than the upper part.

In summary, layering measurements showed sub-horizontal to slightly inclined strata (Sect. 4.2.1, 4.2.2). Weathering visibly affected layering (destabilised slopes where weathering was most active).

The error propagation is indicated by DTM accuracies [*Gwinner et al.*, 2009] and the RMS of the measurement tool itself (Sect. 3.2.3). The accuracy of the elevation model (DTM) was calculated in order to determine the mean square error of the strike and dip. The determination of the accuracy is based on two points (initial and endpoint) on a linear relationship; the lateral deviation was defined.

Here error propagation is shown exemplarily for Iani 3, since it is comparable within the ILDs considering the error of the DTM as mentioned above.

α:	measured strike	240°
γ:	measured dip	4°
RMS $_\alpha$:	measured root mean square of α	22
RMS $_\gamma$:	measured root mean square of γ	2
X, Y:	horizontal accuracy of the DTM	50 m
Z:	vertical accuracy of the DTM	12.5 m
σ_X, σ_Y:	calculated error of the DTM considering X and Y	70.7 m
σ_Z:	calculated error of the DTM considering Z	17.7 m

$$\sigma_X = \sqrt{\left(2 \cdot X^2\right)} \quad \sigma_Y = \sqrt{\left(2 \cdot Y^2\right)} \quad \sigma_Z = \sqrt{\left(2 \cdot Z^2\right)} \tag{VII}$$

x:	sample difference	4300 m
y:	line difference	22850 m

s:	trace length	23251 m
z:	elevation difference	378 m

$$s = \sqrt{x^2 + y^2} \tag{VIII}$$

$\frac{d\alpha}{dx}, \frac{d\alpha}{dy}, \frac{ds}{dx}, \frac{ds}{dy}, \frac{d\gamma}{ds}, \frac{d\gamma}{dz}$: 1st derivation of arc tangent

e.g. arctan' $\frac{x}{y} = \left[\frac{1}{1+\left(\frac{x}{y}\right)^2}\right] \cdot \frac{1}{y}$ (IX)

σ_s: calculated error of the DTM considering *s*
σ_z: calculated error of the DTM considering *z*

$$\sigma_s = \sqrt{\left(\frac{ds}{dx}\right)^2 \cdot \sigma_x^2 + \left(\frac{ds}{dy}\right)^2 \cdot \sigma_y^2} \tag{X}$$

σ_α: calculated error of the DTM considering α
σ_γ: calculated error of the DTM considering γ

$$\sigma_\alpha = \sqrt{\left(\frac{d\alpha}{dx}\right)^2 \cdot \sigma_x^2 + \left(\frac{d\alpha}{dy}\right)^2 \cdot \sigma_y^2} \qquad \sigma_\gamma = \sqrt{\left(\frac{d\gamma}{dz}\right)^2 \cdot \sigma_z^2 + \left(\frac{d\gamma}{ds}\right)^2 \cdot \sigma_s^2} \tag{XI}$$

σ_α was determined ±0.003 and σ_γ was calculated ±0.044.

$$\sigma_{\alpha total} = \sqrt{\left(\sigma_\alpha^2 + RMS_\alpha^2\right)} \qquad \sigma_{\gamma total} = \sqrt{\left(\sigma_\gamma^2 + RMS_\gamma^2\right)} \tag{XII}$$

The total error ($\sigma_{\alpha total}$, $\sigma_{\gamma total}$) of the measurement is consistent with the measured RMS which is $\alpha = 240 \pm 22$ and $\gamma = 4 \pm 2$.
On the whole, the error resulting from the elevation model is very low (0-0.2) for all measured ILDs (Iani3, Ganges 1, Capri/Eos) and thus can be disregarded. On the other hand, the calculated strike and dip (solely based on the DTM) deviates much from the measured values. It should be more accurate since it is only based on two points and thus the variance is much lower than if based on a higher number of points. Consequently, the determination solely based on the DTM is more accurate but considers only two points.

The error for the slopes was calculated similarly by only considering γ and thus determining σ_γ.
Using a DTM with the same resolution as abovementioned errors are

$\gamma = 6 \pm 1$ for low slopes	and $\gamma = 32 \pm 3$ for steeper slopes (and a different s/z-ratio)
s = 1011.2 m	
x = 1000 m	
y = 150 m	
z = 17 m	z = 60 m

5.8 STRATIGRAPHIC RELATIONSHIP AND AGE

ILDs clearly postdate chaotic terrains (e.g. Fig. 41E) because they are present on pre-existing jumbled terrain (e.g. Fig. 43A). As outflow channels emanating from the chaotic terrains are dated to the Late Hesperian/Early Amazonian [*Head et al.*, 2001] ILDs have to be younger [*Scott and Tanaka*, 1986; *Tanaka and Scott*, 1987; *Lucchitta*, 1990; Sect. 2.4.2, 2.2.2, Table 3, 4]. Indeed, observations show that ILDs are younger than the Valles Marineris and the chaotic terrain but older than the landslides overlapping them and the windblown materials (dust, ripples; Sect. 5.1, 5.5) that mostly cover their surface (Sect. 2.4). ILD material apparently deposited conformably upon the irregular chaotic terrain surface (e.g. Fig.36A).

In this study age dating was performed on HRSC nadir images (Table 23). Ages could be obtained for Aram (central part of the ILD), Aureum 1+2, Iani 1-3, and Ganges 1-4 and are shown in Fig. 72. The age of Aram was measured Early Amazonian. For Ganges 1-4 a Middle Amazonian age was estimated and for Aureum 1+2 and Iani 1-3 a Late Amazonian age (Fig. 72). These young, Amazonian ages measured on ILD surfaces raise questions and convene with the mineralogical history shown in figure 3 since most ILDs are sulphate-bearing and sulphates were assumed to have formed during the Hesperian when large amounts of water were present on the Martian surface (Sect. 2.2.2, Table 4). Since ILDs show strong erosional features (Sect. 5.1) and erosion was more intense in the Hesperian, the estimated ages most likely correspond to exposure ages but not to depositional ages. Ganges 1 potentially had a much higher extent in the past, which is possibly indicted by the ages.

Table 24: Age dating performed in this study and in comparison. Note differences in the ages arise in data resolution[1].

Locality	Age [Ga]	Reference
Aram (central part)	2.69	This work
Aram (central and eastern part)	0.3 and 0.07 0.1 (resurfacing)	Rossi et al. (2008)
Aureum 1+2	0.47	This work
Iani 1+2	0.04	This work
Iani 3	0.24	This work
Iani 1+3	0.01 (resurfacing)	Rossi et al. (2008)
Ganges 1	0.94	This work
Ganges 2-4	1.66	This work

[1] *Rossi et al.* (2008) used the higher resolution of MOC-images contrary to HRSC-images used in this study. Discrepancies thus may be explained by the data base. Besides, in this study the whole ILD surface was used for dating while *Rossi et al.* (2008) dated a smaller area (Sect. 2.3.4).

Aureum 1+2

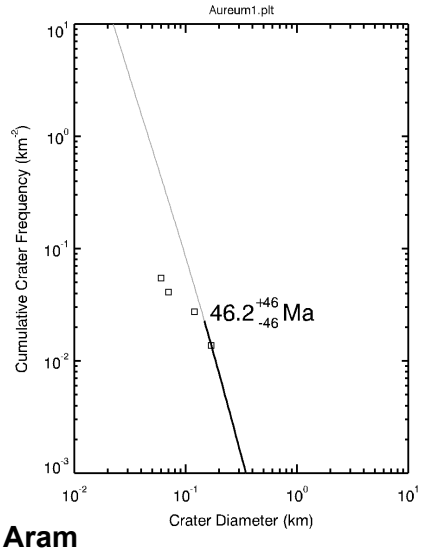

Iani 1+2

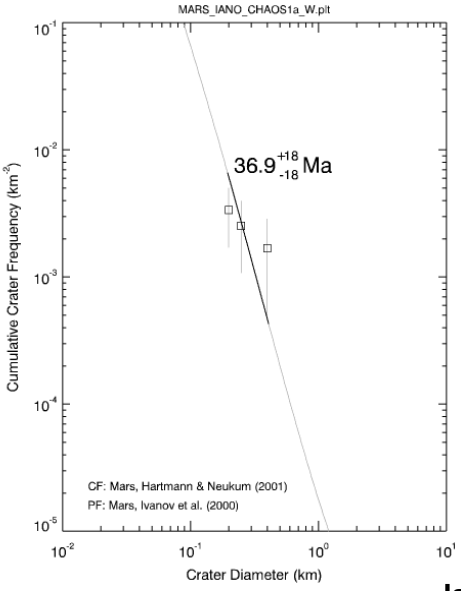

Aram

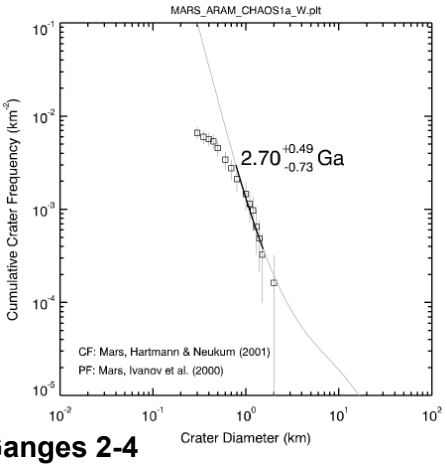

Iani 3

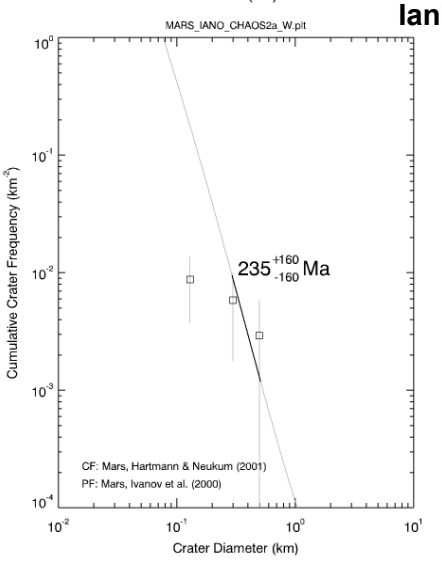

Ganges 2-4

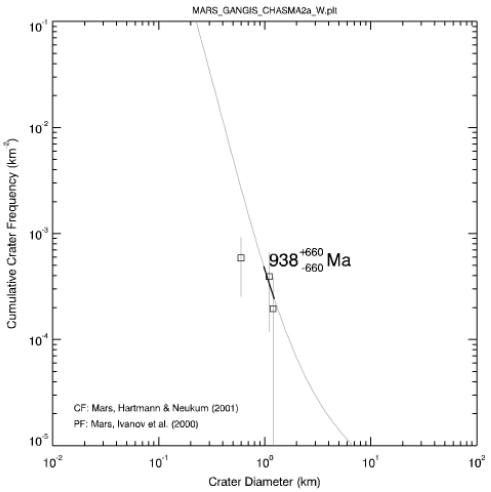

Ganges 1

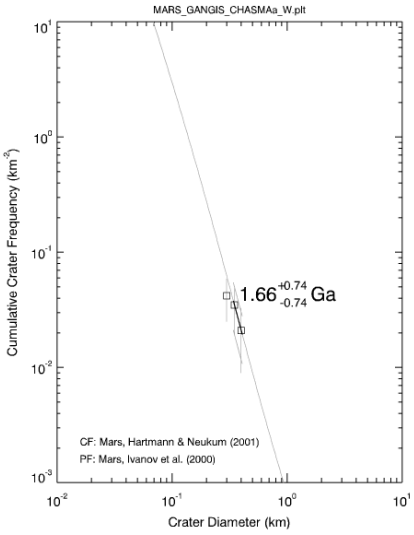

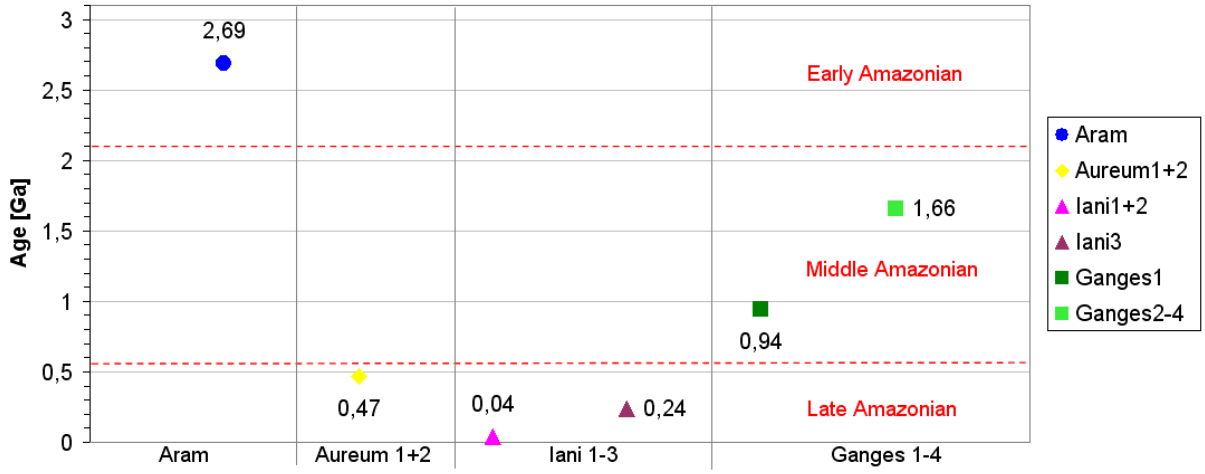

Figure 72: Crater size-frequency dating (Sect. 2.3.4). In order to constrain surface ages measurements were performed. It shows that ILDs resemble a young age due to the rareness of impact craters on their surfaces, potentially erosional ages (Sect. 5.1, 5.5) and *(top)* Layer measurements for the respective ILDs (Aram, Iani 1-3, Aureum 1+2, Ganges 1-4. *(bottom)* Diagram showing all data measured in this study.

As seen in Sect. 2.4.3, age dating confirms a Late Hesperian and Amazonian origin [*Lucchitta*, 1999; *Neukum et al.*, 2007], whereas for Juventae Chasma – located west of the research area at 3.5°S/258.6°E (Fig. 2, Sect. 2.4.3) - an additional age of less than 0.4 Ga (Late Amazonian, Table 3) was measured by *Neukum et al.* (2007). *Rossi et al.* (2008) found young exposures less than 0.3 Ga in age (Late Amazonian, Fig. 11, Table 3) on ILDs in chaotic terrains (Sect. 2.4.3). Aram (Sect. 4.1.1) shows an age of 0.3 Ga and 0.07 Ga (Late Amazonian, Table 3). Moreover, it has been ascertained (Sect. 2.4.3) that Iani 1+3 (Sect. 4.1.3) experienced a resurfacing event around 0.01 Ga ago (Table 3). This resurfacing event is assumed to have affected the ILDs located within 200 km from each other.

ILD ages estimated here (Fig. 72) are comparable to those measured by other workers [*Neukum et al.*, 2007; *Rossi et al.*, 2008] in indicating Amazonian ages.

In detail, here (Fig. 72) the central part of the Aram ILD (Fig. 29) was measured Early Amazonian while *Rossi et al.* (2008) derived a Late Amazonian age for both, central and eastern part. This discrepancy between central and eastern part could indicate the eastern part of Aram experienced stronger erosion and suggesting material that is more susceptible to erosion than that in the central part, which is possibly explained by the lack of a protecting unit 2 (capping unit; Fig. 31B, Sect. 4.1.1) in the eastern part. Since hydrated sulphates were found within unit 1 (Fig. 72) which are in the eastern part of Aram not protected by a capping unit (unit 2), erosion apparently is more successful on the weak unprotected sulphate-rich rocks.

Ganges 1 shows a lower age of 0.94 Ga than Ganges 2-4 which was estimated 1.66 Ga (Fig. 72). This could indicate erosion was stronger on the surface of Ganges 1 than on Ganges 2-4 which could be (1) an effect of elevation – (Ganges 1 is -500 m vs. Ganges 2+3 are -4800 m and Ganges 4 is -4800 m high, Fig. 72) – and the resulting wind regime or (2) it could indicate different material since at least Ganges 2+4 (Fig. 72) neither indicate hydrated minerals nor iron-rich minerals whereas Ganges 1 shows hydrated sulphates (Fig. 72) that could be more susceptible to erosion.